Measurement of Gross Photosynthesis, Respiration in the Light, and Mesophyll Conductance Using $H_2{}^{18}O$ Labeling[1][OPEN]

Paul P. G. Gauthier,[a,2] Mark O. Battle,[b] Kevin L. Griffin,[c,d] and Michael L. Bender[a,e]

[a]Department of Geosciences, Princeton University, Princeton, New Jersey 08544
[b]Department of Physics and Astronomy, Bowdoin College, Brunswick, Maine 04011
[c]Department of Earth and Environmental Sciences, Columbia University, New York, New York 10027
[d]Department of Ecology, Evolution, and Environmental Biology, Columbia University, New York, New York 10027
[e]Institute of Oceanology, Shanghai Jiao Tong University, Shanghai, China

ORCID ID: 0000-0002-2893-7861 (P.P.G.G.).

A fundamental challenge in plant physiology is independently determining the rates of gross O_2 production by photosynthesis and O_2 consumption by respiration, photorespiration, and other processes. Previous studies on isolated chloroplasts or leaves have separately constrained net and gross O_2 production (NOP and GOP, respectively) by labeling ambient O_2 with ^{18}O while leaf water was unlabeled. Here, we describe a method to accurately measure GOP and NOP of whole detached leaves in a cuvette as a routine gas-exchange measurement. The petiole is immersed in water enriched to a $\delta^{18}O$ of ~9,000‰, and leaf water is labeled through the transpiration stream. Photosynthesis transfers ^{18}O from H_2O to O_2. GOP is calculated from the increase in $\delta^{18}O$ of O_2 as air passes through the cuvette. NOP is determined from the increase in O_2/N_2. Both terms are measured by isotope ratio mass spectrometry. CO_2 assimilation and other standard gas-exchange parameters also were measured. Reproducible measurements are made on a single leaf for more than 15 h. We used this method to measure the light response curve of NOP and GOP in French bean (*Phaseolus vulgaris*) at 21% and 2% O_2. We then used these data to examine the O_2/CO_2 ratio of net photosynthesis, the light response curve of mesophyll conductance, and the apparent inhibition of respiration in the light (Kok effect) at both oxygen levels. The results are discussed in the context of evaluating the technique as a tool to study and understand leaf physiological traits.

Gross O_2 production (GOP; the rate of water splitting at PSII), mitochondrial respiration in the light (R_L), the oxygenation of Rubisco, and the photosynthetic carbon oxidation cycle (i.e. photorespiration; Hagemann et al., 2013) are fundamental rate properties of plants. When assessed as net O_2 fluxes, the rates of these processes are confounded. Since each of the component processes represents a distinct biochemical pathway with important cellular functions, quantifying the contribution of these processes to the net assimilatory flux is of particular interest. The utilization of O_2 as an electron acceptor around PSI via the Mehler reaction also can contribute to O_2 uptake (Badger et al., 2000). Precise measurements of O_2 fluxes from leaves would provide a better understanding of these important processes and shed light on diverse metabolic responses to environmental variation (Furbank et al., 1982; Badger et al., 2000; Hillier, 2008; André, 2011).

A variety of methods have been developed in leaves and phytoplankton to measure net O_2 production (NOP; Kok, 1948; Cornic et al., 1989; Laisk et al., 1992; Laisk and Oja, 1998). GOP has been measured directly using an ^{18}O tracer and mass spectrometry (Mehler and Brown 1952; Hoch et al., 1963; Ozbun et al., 1964; Radmer and Ollinger, 1980; Ruuska et al., 2000). Two general approaches have been used to measure GOP: (1) measuring the increase of $^{16}O_2$ from unlabeled water in a chamber containing dioxygen only as $^{18}O_2$; and (2) measuring $^{18}O^{16}O$ of photosynthetic O_2, produced from splitting ^{18}O-labeled water. All published GOP data for leaves use the first approach to determine GOP and, given NOP measurements, O_2 uptake (Berry et al., 1978; Gerbaud and André, 1979; Canvin et al., 1980; Peltier and Thibault, 1985; Biehler and Fock, 1995; Haupt-Herting and Fock, 2002; André, 2011). Typically, this method relies on leaf fractions or small leaves that are placed in a gas-tight gas-exchange chamber connected to a membrane inlet mass spectrometer (Berry et al., 1978; Biehler and Fock, 1995). The chamber air is then replaced with O_2 present as $^{18}O_2$, and the evolution of $^{16}O_2$ and $^{18}O_2$ is monitored. The decrease of $^{18}O_2$ concentration in the system constrains O_2 uptake, and the

[1] This work was funded by the Princeton Environmental Institute Grand Challenge Grant Program.

[2] Address correspondence to ppg@princeton.edu.

The author responsible for distribution of materials integral to the findings presented in this article in accordance with the policy described in the Instructions for Authors (www.plantphysiol.org) is: Paul P.G. Gauthier (ppg@princeton.edu).

P.P.G.G. designed the experiments, analyzed the data, and prepared the article; P.P.G.G., M.O.B., K.L.G., and M.L.B. designed the gas-exchange cuvette; M.O.B. built the cuvette; K.L.G. and M.L.B supervised the experiments; all authors discussed the results and worked on the article.

[OPEN] Articles can be viewed without a subscription.

www.plantphysiol.org/cgi/doi/10.1104/pp.16.00741

increase of $^{16}O_2$ gives GOP. GOP, determined in this way, is a reliable measure of the electron transport rate (J; André, 2013), which then can be used to estimate mesophyll conductance (g_m; Flexas et al., 2012) and chloroplastic $[CO_2]$ (C_c; Renou et al., 1990; André, 2011). Nevertheless, among current methods used to measure g_m (for review, see Flexas et al., 2012), the ^{18}O method was limited by a restriction associated with obtaining $^{18}O_2$ and the need for specific equipment (e.g. membrane inlet mass spectrometry). As a consequence, to date, measurements of NOP and GOP have received little attention.

The second approach, relying on ^{18}O-labeled water, has been used to measure NOP and GOP in phytoplankton (Grande et al., 1989; Goldman et al., 2015). With this method, water in the cells is labeled with $H_2{}^{18}O$. If implemented with a whole leaf in a flow-through gas-exchange system, the leaf would be labeled with $H_2{}^{18}O$ via the transpiration stream. In the cuvette, NOP raises the O_2 concentration, and GOP also raises the $\delta^{18}O$ of O_2. The rates of NOP and GOP are measured from the difference in O_2/N_2 (Grande et al., 1989) and $\delta^{18}O$ of O_2 in air entering and leaving the cuvette. O_2 uptake is the difference between these two rates (GOP – NOP). The measurement of the change in O_2 concentration is a standard practice for high-precision measurements: changes in O_2 concentration are routinely measured from changes in the ratio of O_2/N_2 rather than from the O_2 concentration or partial pressure, which also depend on temperature and humidity.

The advantage of this method is that gas-exchange properties are determined with a steady-state gas-exchange protocol rather than in a closed gas-exchange system. The challenge of this technique is that there are only small differences in the O_2/N_2 ratio and $\delta^{18}O$ of O_2 between outgoing and incoming air. These small changes can be measured by high-precision isotope ratio mass spectrometry. For example, a rate of NOP resulting in a CO_2 drawdown or O_2 rise of 100 μL L^{-1} would cause O_2/N_2 in air exiting the chamber to be increased by 0.47‰. If water molecules were labeled to +10,000‰, GOP of 100 μmol mol^{-1} would cause $\delta^{18}O$ of O_2 to increase by 5‰. For comparison, $\delta O_2/N_2$ can be measured by isotope ratio mass spectrometry to a precision of ±0.005‰ and $\delta^{18}O$ of O_2 can be measured to a precision of ±0.03‰ or better (Bender et al., 1994). Thus, one can measure $[O_2]$ and $\delta^{18}O$ changes associated with NOP and GOP to a precision of about ±1 μL L^{-1} out of 210,000 μL L^{-1} (Bender et al., 1998). Our $H_2{}^{18}O$ labeling approach, as described below, allows us to simultaneously measure a full set of fundamental gas-exchange properties, including NOP and GOP. We also can measure light and CO_2 response curves, thus characterizing many important physiological properties of plants simultaneously. As will be shown, we can regulate flow rate, temperature, humidity, and other properties of air in the chamber.

As a demonstration of the utility of this technique, we measured GOP and NOP of French bean (*Phaseolus vulgaris*) as a function of irradiance at 21% and 2% O_2. We also measured CO_2 assimilation. We then used these results to examine $\Delta O_2/\Delta CO_2$ during exposure to light, the light response of g_m, and the Kok effect (apparent inhibition of respiration in the light; Kok, 1948, 1956; Hoch et al., 1963) under normal and non-photorespiratory conditions.

RESULTS

Measurement of Net and Gross Photosynthesis

Gas-exchange equations predict that net assimilation (A_{net}) increases linearly at low light intensity, where light is limiting, and plateaus at high light levels, where CO_2 assimilation is limited by Rubisco activity. In Figure 1, the linear portion of the curve is restricted to light intensities lower than 160 μmol m^{-2} s^{-1}. The asymptote of the photosynthesis light response curve represents the maximum rate of A_{net}, NOP, or GOP. The asymptote is determined using a nonrectangular quadratic function. At 21% O_2, GOP_{max} (the subscript max refers to the asymptotic value) is 34.2 μmol m^{-2} s^{-1} and NOP_{max} is 13.5 μmol m^{-2} s^{-1}. At 2% O_2, GOP_{max} is 19 μmol m^{-2} s^{-1} and NOP_{max} is 15.8 μmol m^{-2} s^{-1}. At any given $[O_2]$, NOP_{max} and A_{max} are indistinguishable, as also suggested by Figure 2. The difference between GOP and NOP at 21% O_2 is greatest at maximum light intensity. This point corresponds to a reduction in C_i values (Supplemental Fig. S1). In this discussion, we acknowledge that ambient CO_2 (C_a) changed in the leaf chamber (Supplemental Fig. S1). During the experiments at 21% O_2, C_i increases from 245 ± 5 μmol mol^{-1} at maximum light intensity to 458 ± 8 μmol mol^{-1} in darkness. The variation in C_i with irradiance is a consequence of changes in net photosynthesis and respiration as well as variable stomatal closure and C_a in the cuvette (from 379 ± 4 to 426 ± 3 μmol mol^{-1}). As a consequence, C_a is slightly higher in the dark, where respiration adds CO_2 to ambient air, than in the light, where photosynthetic assimilation removes CO_2. The ambient CO_2 in the cuvette depends on the difference between net CO_2 assimilation by the leaf and the flux of CO_2 into the cuvette. At 2% O_2, C_i increases with decreasing light intensity. The range of increase is enhanced by the higher gross assimilation rate at high irradiances (from 129 ± 19 to 437 ± 13 μmol mol^{-1}). For irradiances above 200 μmol photosynthetically active radiation (PAR) m^{-2} s^{-1} at 2% O_2, C_i was lower than 200 μmol mol^{-1} and considered limiting for photosynthesis. The discussion of the results focuses on the lower irradiance range (0–200 μmol PAR m^{-2} s^{-1}).

All measured responses of GOP to increasing light intensities follow a similar nonrectangular quadratic function (Fig. 1, C and D). As suggested by the higher SD of fluxes in the replicate experiments (Fig. 1), GOP is most variable from leaf to leaf at high light intensities. However, this variability is less pronounced for measurements at 2% O_2 (Fig. 1). Nevertheless, the precision of the measurements is better at 2% than at 21% O_2 (for

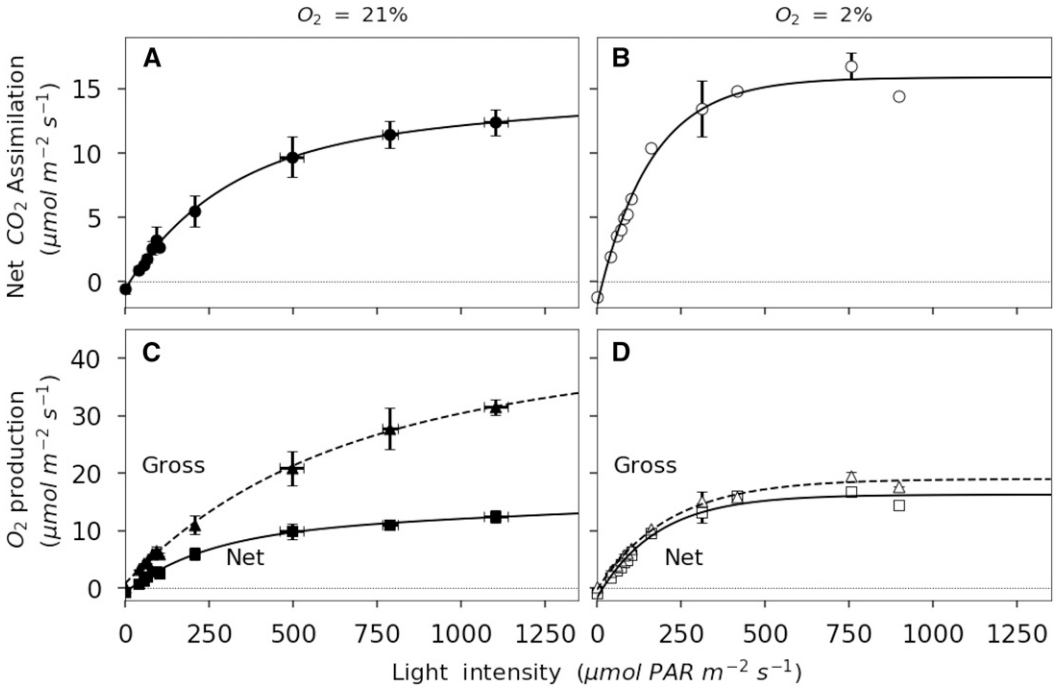

Figure 1. Light response of net CO_2 assimilation and NOP for French bean leaves exposed to 21% O_2 (black symbols) or 2% O_2 (white symbols). A and B, Light responses of net CO_2 assimilation. C and D, Light responses of NOP. Nonrectangular quadratic curves are represented by solid lines for net fluxes and by dashed lines for GOP. Errors bars represent SE for $n = 3$.

description about $d^{18}O$ accuracy and precision, see Supplemental Material).

Figure 2 shows a positive correlation of nearly 1:1 between NOP and A_{net}. At 21% O_2, the linear regression between NOP and A_{net} (photosynthetic quotient) is 1.066 ± 0.013 (r^2 = 99.6%, $P < 0.01$) O_2 per CO_2. At 2% O_2, it is 0.978 ± 0.013 (r^2 = 99.5%, $P < 0.01$) O_2 per CO_2. The ratio NOP/A_{net} for values obtained in the linear portion of the curve (light intensities lower than 160 μmol m^{-2} s^{-1}) is 0.982 ± 0.097 (r^2 = 90.2%, $P < 0.01$) at 21% O_2 and 0.956 ± 0.013 (r^2 = 99.5%, $P < 0.01$) at 2% O_2. The correlation between NOP and A_{net} in the Rubisco-limited part of the curve (light intensity above 160 μmol m^{-2} s^{-1}) is 1.026 ± 0.027 (r^2 = 99.2%, $P < 0.01$) O_2 per CO_2 at 21% O_2 and 0.999 ± 0.067 (r^2 = 97.3%, $P < 0.01$) O_2 per CO_2 at 2% O_2. The correlation between NOP and A_{net} for all the data presented in Figure 2 is 1.006 ± 0.012 (r^2 = 99.1%, $P < 0.01$). This correlation validates the measurement of net photosynthesis using either O_2 or CO_2 fluxes.

Stomatal Conductance and g_m

Stomatal conductance (g_s) increases with light intensity to reach a maximum around 0.1 mol m^{-2} s^{-1} (Fig. 3A), but g_s is higher at 2% O_2 than at 21% O_2. Light saturation of g_s occurs at about 160 μmol PAR m^{-2} s^{-1} at 2% O_2 and 500 μmol PAR m^{-2} s^{-1} at 21% O_2.

At 21% O_2, g_m increases with irradiance to an asymptotic value. As irradiance rises above about 110 μmol m^{-2} s^{-1}, C_c decreases slightly from 161 ± 16 to 109 ± 5 μmol mol^{-1} (Fig. 3, B and C). Nevertheless, C_c tends to be conserved, and variation in C_i seems to be compensated for by an increase of g_m with increasing light intensities. In fact, g_m reaches an asymptote by 400 to 450 μmol PAR m^{-2} s^{-1}. At 21% O_2, this asymptote is around 0.1 mol CO_2 m^{-2} s^{-1}. At 2% O_2, because O_2 uptake is similar to R_L, g_m and C_c cannot be calculated (see Eq. 18 in "Materials and Methods").

The Kok Effect under Photorespiratory and Nonphotorespiratory Conditions

Considering the light-limited part of the experiment, Figure 4 summarizes the data for the linear portion of the light response curve. Linear regression of GOP and NOP in the low-light-intensity part of the photosynthesis-irradiance curve (0–160 μmol PAR m^{-2} s^{-1}) is used for leaves exposed to either 21% or 2% O_2. At 21% O_2, the linear portion of the curve occurs between 0 and 90 μmol PAR m^{-2} s^{-1}. At 21% O_2, NOP and GOP diverge as light intensities rise, reflecting increasing photorespiration at higher rates of A_{net} or GOP. The slope of GOP versus irradiance for values between 0 and 110 μmol m^{-2} s^{-1} is 0.07 ± 0.004 μmol O_2 produced per quanta (r^2 = 98.2, $P < 0.01$) at 21% O_2. The slope of NOP is 0.054 ± 0.002 O_2 molecules produced per quanta (r^2 = 99.7%, $P < 0.01$). The linear portion of GOP and NOP versus irradiance curves at 2% O_2 lies below 110 μmol m^{-2} s^{-1}. At 2% O_2, the slopes of GOP

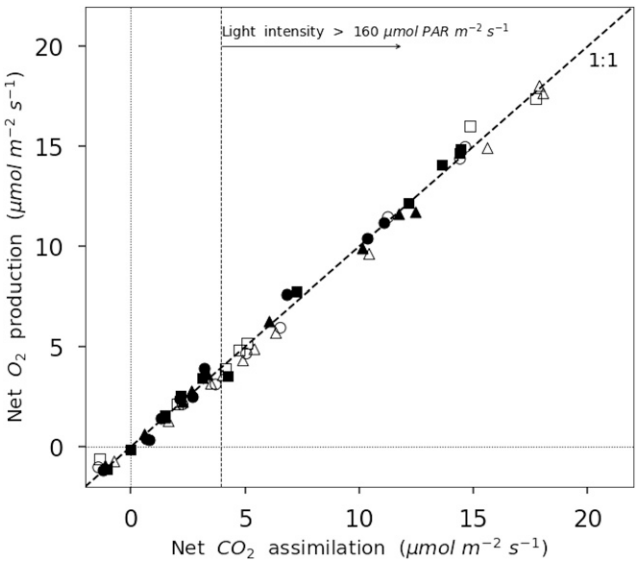

Figure 2. Correlation between NOP and net CO_2 assimilation for leaves exposed to 21% O_2 (black symbols) or 2% O_2 (white symbols). The dashed line represents a 1:1 relation.

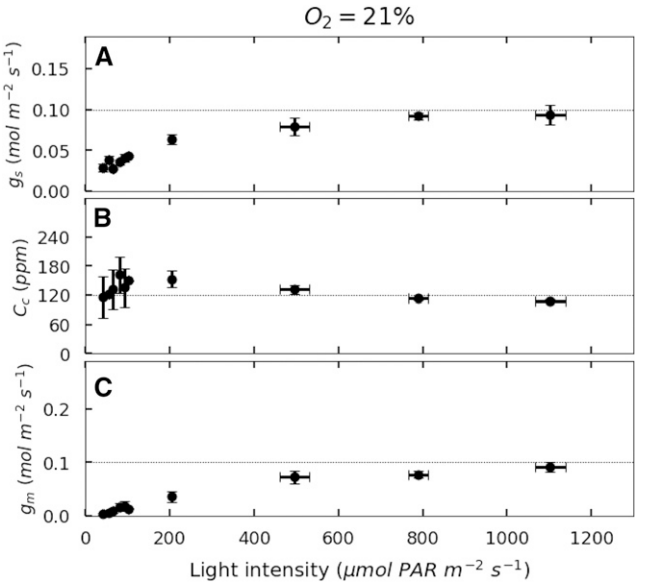

Figure 3. Light response of g_s, C_c, and g_m for French bean leaves exposed to 21% O_2. A, g_s. B, C_c. C, g_m. Dotted lines represent asymptotic values for each parameter. Errors bars represent SE for $n = 3$.

and NOP with increasing light intensities were similar, 0.066 ± 0.002 O_2 molecules produced per quanta (r^2 = 99.7, $P < 0.01$).

Similarly, using linear regressions of the NOP and A_{net} values obtained for light intensities in the linear portion of the NOP and A_{net} light response curves above 35 μmol PAR m^{-2} s^{-1} (as defined above) for individual leaves, a rate of respiration in the light can be obtained following the Kok method. On average, R_o-apparent is 0.54 ± 0.16 μmol m^{-2} s^{-1}. In comparison, the averaged value of dark respiration (R_{dark}) is 1.06 ± 0.07 μmol m^{-2} s^{-1}. As a consequence, R_o-apparent for 21% O_2 is inhibited by 46% at light intensities above the break point in the light response curve. At 2% O_2, linear regressions of GOP and NOP against irradiance are parallel (Fig. 4B), and the linear regression of NOP intercepts the y axis at the average value of dark respiration (R_{dark} = 0.79 ± 0.12 μmol m^{-2} s^{-1}). Therefore, at 2% O_2, there is no discernible Kok effect and no apparent light inhibition of mitochondrial respiration.

Dark respiration values (1.06 ± 0.07 μmol m^{-2} s^{-1} at 21% O_2 and 0.79 ± 0.12 μmol m^{-2} s^{-1} at 2% O_2) are compared with R_o-corrected or R_c-corrected values calculated from either O_2 or CO_2, respectively (Fig. 5). At 21% O_2, the C_i correction increases R_o slightly from 0.59 ± 0.05 to 0.68 ± 0.04 μmol m^{-2} s^{-1}. Thus, after correction, respiration is 36% lower in the light than in the dark. For R_c, the apparent value is 0.74 ± 0.14 μmol m^{-2} s^{-1} and the corrected value is 0.64 ± 0.04 μmol m^{-2} s^{-1}. Although the impact of the C_i correction on the true values of R_o and R_c are different, at 21% O_2, these differences are not statistically significant using a Student's t test comparison with $P > 0.05$. At 2% O_2, the correction for C_i variations decreases R_c from 1.15 ± 0.39 to 0.64 ± 0.04 μmol m^{-2} s^{-1} and decreases R_o from 0.86 ± 0.28 to 0.72 ± 0.04 μmol m^{-2} s^{-1}. The respiratory quotient for apparent respiration in the light is then 1.06 ± 0.14 at 21% O_2 and 1.12 ± 0.05 at 2% O_2.

DISCUSSION

Assessment of the Gas-Exchange Method

The technique developed here is a robust gas-exchange method combining cavity ring-down spectrometers (CRDS) with a high-precision isotope ratio mass spectrometer (IRMS) to more fully characterize leaf carbon, oxygen, and water vapor exchanges under near-ambient conditions. This technique takes advantage of the ability of the IRMS to achieve a precision of ±0.03‰ in the measurement of $\delta^{18}O$ and ±0.005‰ in $\delta O_2/N_2$. This technique does not enable the measurement of previously unmeasured properties. For example, GOP has been measured before by $^{18}O_2$ labeling (Berry et al., 1978; Canvin et al., 1980; Peltier and Thibault, 1985; Biehler et al., 1997; Badger et al., 2000; Haupt-Herting and Fock, 2000; Ruuska et al., 2000). However, our technique has two main virtues. First, the use of a steady-state gas-exchange system allows the measurement of leaf properties such as R_L and g_m that could not be easily measured in the closed-system chambers used previously to measure GOP. Second, this instrument allows us to constrain and vary major environmental properties such as O_2 concentrations, irradiance, and temperature in a systematic way and, thus, to study a variety of leaf physiological processes.

Compared with previously used closed gas-exchanges systems (Laisk et al., 1992; Badger et al., 2000; Haupt-Herting and Fock, 2002), the technique

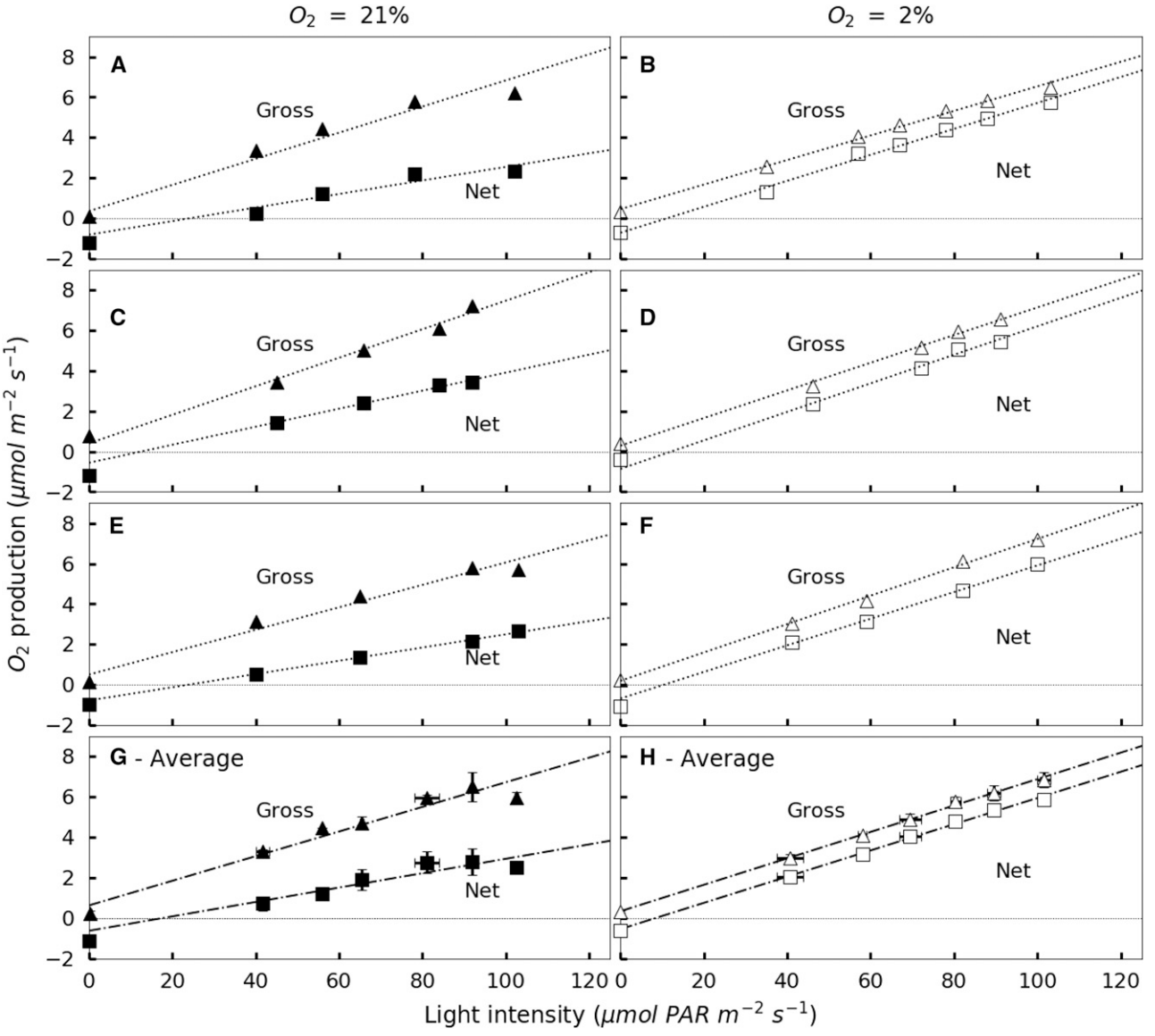

Figure 4. Low-light response of NOP (squares) and GOP (triangles) for individual leaves of French bean exposed to 21% O_2 (black symbols) or 2% O_2 (white symbols). A through F show individual low-light responses, and G and H show averaged values. NOP values are corrected for C_i variation using Kirschbaum and Farquhar (1987). Dashed-dotted lines represent the linear regression of the values obtained for light intensities between 40 and 100 μmol m^{-2} s^{-1}. Error bars represent SE for $n = 3$.

developed here presents significant improvements that overcome several previous limitations. However, special care needs to be taken when preparing detached leaves. Detaching leaves from their main branch can disrupt the continuity of the water stream and lead to xylem embolism and leaf wilting (Savvides et al., 2012; Tombesi et al., 2014). As in Gauthier et al. (2010), where detached leaves were maintained alive for up to 16 h, the protocol described here (see above) routinely allowed measurements for more than 15 h. In past experiments using membrane inlet mass spectrometry, the cost of $^{18}O_2$ limited the length of experiments to only a few hours (Atkins and Canvin, 1971; Harris et al., 1983), also limiting the range of measurements and their application. The technique presented overcomes this limitation by using ambient air and a limited amount of $H_2{}^{18}O$. Second, the utilization of entire leaves has two advantages: it limits leaf desiccation (Flexas et al., 2006) and reduces stress reactions associated with leaf cutting. Furthermore, it increases the difference between entering and exiting air and increases repeatability and precision (Supplemental Figs. S4 and S5). Finally, compared with the techniques used on attached leaves, enclosing a leaf, petiole, and water supply reduces potential system leaks (Yakir, 1992; Haupt-Herting and Fock, 2000).

The limitations associated with working on detached leaves also need to be recognized. There is evidence that

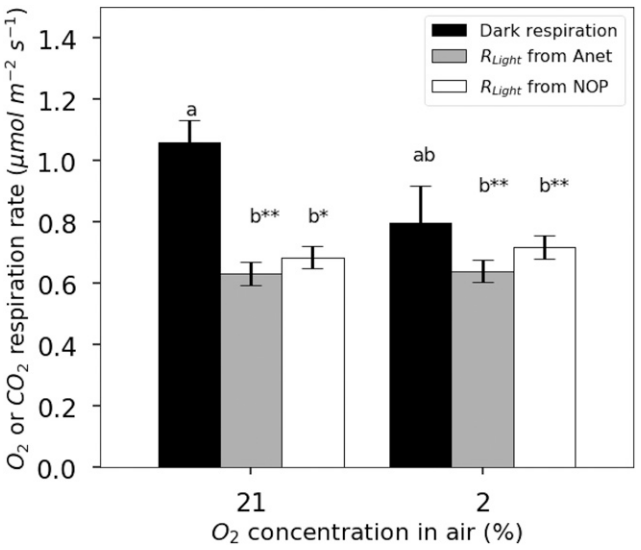

Figure 5. Comparison of respiration rates measured in the dark (black bars) and apparent respiration rate in the light using the Kok method on A_{net} (gray bars) or using the Kok method on NOP (white bars) for French bean leaves exposed to 21% O_2 or 2% O_2. Values of R_{Light} were corrected for variations in C_i. Results of Student's *t* test are represented by double asterisks when the difference from the other group is very significant ($P \leq 0.01$) and by single asterisks at $P < 0.05$. Each group is represented by a different letter, a or b. Error bars represent SE for $n = 3$.

g_s is regulated by water potential and plant water status (Buckley, 2017), yet in our experiments here, leaf water potential was not monitored. Thus, the low g_s and resulting C_i observed in our experiments may be associated with detaching the leaves. Alternatively, the low g_s also could have been generated by stomatal patchiness (Buckley et al., 1997; Mott and Buckley, 2000). Finally, we note the limitation associated with variable C_a inside the chamber, which led to limiting C_i values (less than 200 μL L^{-1}) under nonphotorespiratory conditions. This limiting C_i could lead to a limitation of carbamylation and the apparent inactivation of Rubisco (Sage et al., 2002). Future experiments should continue to quantify and minimize the overall stomatal response while attempting to study leaf physiological parameters under near-ambient conditions and constant C_a.

This system enables the measurement of GOP and NOP concurrently with many other commonly measured properties, such as A_{net}, g_s, and carbon isotope discrimination. There are a number of ways in which this instrument could be applied to important topics in plant physiology. For example, the measurement of GOP and electron flow through the photosynthetic electron transport chain also can be used to quantify the quantum yield of photosynthesis if light absorption is measured (Singsaas et al., 2001). Similarly, precise measurements of GOP coupled with NOP can constrain O_2 uptake and provide some insight into the role of the Mehler reaction (Badger et al., 2000; Haupt-Herting and Fock, 2002). Finally, GOP can be compared directly with fluorescence, which is its proxy for electron flow (Genty et al., 1989; von Caemmerer, 2000; André, 2011). Calibrating fluorescence against measured values of GOP would allow accurate estimates of this property in a wide range of studies.

NOP data, together with measurements of A_{net}, allow us to determine the stoichiometry of photosynthesis and respiration, expressed as $\Delta O_2/\Delta CO_2$. Doing so adds the capacity to assess processes such as nitrate assimilation (Bloom et al., 1989), anaplerotic carbon fixation (Oja et al., 2007; Angert et al., 2012), or the production of lipids (Aubert et al., 1996; Devaux et al., 2003; Tcherkez et al., 2003), in addition to potential changes in the respiratory substrates and cellular energetics (Tcherkez et al., 2003; Nogués et al., 2004). In our experiments, the photosynthetic quotient was nearly constant and very close to 1, as seen by the strong 1:1 relationship between NOP and A_{net} (Fig. 2). This is to be expected if both the photosynthates created and the respiratory substrates used during the measurement were Glc, starch, and other basic carbohydrates. However, considering the low rate of R_L, the influence of the respiratory substrates on the net assimilation quotient is relatively small. In addition, the ratio NOP/A_{net} at 21% O_2 was slightly higher than 1 by a few percent. This small imbalance in O_2 production compared with CO_2 assimilation could emerge from O_2 produced during nitrogen assimilation in leaves (Bloom et al., 1989). In addition, we are mindful that, in low light, calculations of $\Delta O_2/\Delta CO_2$ due to respiration in the light from CO_2 and O_2 exchange are inherently uncertain. This is because they rely on extrapolating NOP and A_{net} to zero irradiance. Although photosynthesis and respiratory quotients of leaves are rarely measured in gas-exchange experiments, they have the potential to add valuable information. As discussed here, with our system, it is possible to measure these properties under a variety of ambient conditions.

Response of g_m to Light Intensity

Measuring GOP allows for the calculation of both C_c and g_m (Renou et al., 1990; André 2011; Flexas et al., 2012). We found, in French bean, that g_m doubled when light increased from 200 to 1,100 μmol PAR m^{-2} s^{-1}. Similar responses have been reported previously from C isotope discrimination ($\Delta^{13}C$; Hassiotou et al., 2009; Douthe et al., 2011, 2012) or fluorescence measurements (Flexas et al., 2007; Xiong et al., 2015). Douthe et al. (2011) found that, when light increased from 200 to 1,100 μmol PAR m^{-2} s^{-1}, g_m increased by 60% for three *Eucalyptus* spp. In a similar light intensity range, Flexas et al. (2007) found a 40% increase of g_m with irradiance for *Olea* and *Vitis* spp. Finally, Hassiotou et al. (2009) reported an increase with irradiance of 22% of g_m in six species of *Banksia*. The response of g_m to irradiance is likely to be species dependent and may be a strategy for plants to maintain a positive carbon balance in leaves (Flexas et al., 2006). However, no consensus exists

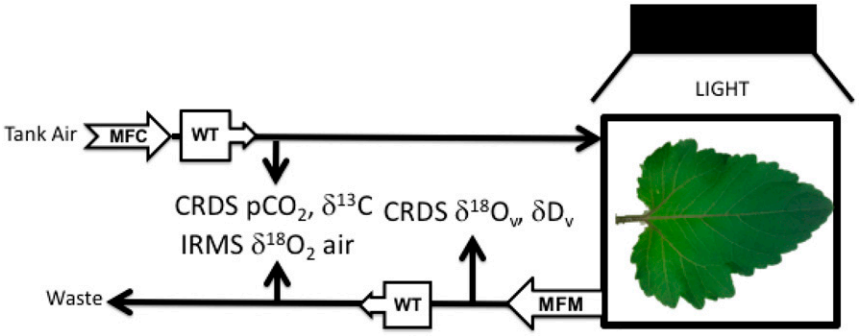

Figure 6. Schematic of the gas-exchange system used for the experiments. MFC, Mass flow controller; WT, water trap; CRDS, cavity ring-down spectrometer; IRMS, isotope ratio mass spectrometer; MFM, mass flow meter. Subscript *v* is water vapor.

regarding the mechanism for the rapidity of the response (Douthe et al., 2011). Our results demonstrate the capacity of our system to determine g_m, adding to the short list of studies using alternative approaches to the most commonly used techniques (fluorescence or ^{13}C) to study environmental responses of g_m.

Major differences exist between previously reported g_m methods and the current O_2 method. The O_2 method has some distinct advantages for studying g_m responses to environmental factors. Carbon isotope approaches use a combination of isotope effects associated with carbon metabolism (Tazoe et al., 2011) to estimate g_m. The relevant fractionation processes that need to be considered include the diffusion of CO_2 through the stomata (a = 4.4‰), the fractionation for dissolution and diffusion through water (a_1 = 1.8‰), fractionation caused by Rubisco (b = 30‰), and fractionation associated with respiration and photorespiration (e = 5.1‰ and f = 11.6‰, respectively; Gong et al., 2015). g_m is then calculated according to Tazoe et al. (2011):

$$g_m = \frac{\left(b - a_1 - \frac{eR_L}{A_{net}+R_L}\right)\frac{A_{net}}{p_a}}{a + \frac{(b-a)p_i}{p_a} - \Delta_{obs} - \frac{eR_L\left(p_i - \Gamma^*\right)}{(A_{net}+R_L)p_a} - \frac{f\Gamma^*}{p_a}} \quad (21)$$

where A_{net} is net CO_2 assimilation, p_i and p_a are CO_2 partial pressure of the ambient and intercellular airspaces, Γ^* is the compensation point in the absence of R_L, and Δ_{obs} is the observed CO_2 discrimination calculated from the difference in C isotopes entering and leaving an open gas-exchange system (Evans et al., 1986). Photorespiratory and respiratory fluxes are determined using Γ^* and R_L. By making these measurements at 2% O_2, the impact of R_L and Γ^* on the estimate of g_m remains small and negligible (Tazoe et al., 2009). Comparing Equations 18 and 21, we can see that both equations constraining g_m invoke four common terms: R_L, A_{net}, Γ^*, and C_i. The O_2 method also requires determining $U - R_L$, while the ^{13}C method requires estimating five isotope effects and the apparent discrimination (Δ). Furthermore, Gong et al. (2015) have shown that differences in the $\delta^{13}C$ between the tank gas used in gas-exchange experiments and the ambient air the plants were grown in can lead to errors in calculated values of photosynthetic discrimination. This problem is avoided when using the O_2 method, where the only unique term needed to calculate g_m is U (Eq. 16), determined from measurements of GOP and NOP. The main assumption of the O_2 method is that oxygen consumption is negligible for processes other than photorespiration and respiration (such as photoreduction by chlororespiration or the Mehler reaction). Finally, Equation 21 has been shown to overestimate g_m (Farquhar and Cernusak, 2012), and the ternary effect of transpiration rate on A_{net} needs to be considered for the estimates of g_m using the ^{13}C method.

Mitochondrial Respiration in the Light

We found that, at 21% O_2, respiration was light inhibited (based on the nonlinearity in the light response curve of A_{net}), as has been commonly found in other experiments (Atkin et al., 2005; Tcherkez et al., 2008; Heskel et al., 2013). However, at 2% O_2, light did not inhibit mitochondrial respiration (i.e. there was no Kok effect). The lack of a Kok effect under ambient [CO_2] has been found previously in studies of maize (*Zea mays*; Cornic and Jarvis 1972) and rice (*Oryza sativa*; Ishii and Murata, 1978). In the case of maize, a C4 plant where photorespiration is insignificant, Cornic and Jarvis (1972) measured the light response curve at low irradiances using 0%, 21%, and 100% O_2 and did not observe a Kok effect. They concluded that the lack of a Kok effect could be explained by the lack of photorespiration under natural conditions. For rice, Ishii and Murata (1978) did not observe a Kok effect at 2% O_2 but observed a larger Kok effect with 50% O_2. This led them to conclude that photorespiration was the proximate cause of the Kok effect.

However, contrary to the two studies on maize and rice, Sharp et al. (1984) found the occurrence of a Kok effect in sunflower (*Helianthus annuus*) leaves under elevated [CO_2]. Since photorespiration is inhibited under high CO_2, the explanation of a direct influence of photorespiration on the Kok effect may be too simple. Sharp et al. (1984) also reported a reduction of dark respiration under low O_2. However, they suggested that it originated from the limitation of O_2 uptake by the mitochondrial electron transport chain when O_2 was less than 2% (their low-O_2 partial pressures were 1%).

Our data also suggested a lower dark respiration rate at 2% O_2, but the difference was not statistically significant (Student's t test, $P = 0.056$). Furthermore, Griffin and Turnbull (2013) and Yin et al. (2011) reported significant light inhibition of respiration in both C3 and C4 plants. Tcherkez et al. (2008) found that the inhibition of respiration in the light is independent of the CO_2/O_2 ratio but that, under low-O_2 conditions, the degree of inhibition may diminish. More recently, Farquhar and Busch (2017) suggested that most of the Kok effect could be explained by a variation in C_c under limiting irradiances. However, in *Vicia faba*, this explanation was not confirmed. Instead, Buckley et al. (2017) found that (1) the break point (Kok effect) was unaffected by $[O_2]$, confirming the findings of Tcherkez et al. (2008), and (2) the activity of the oxygen components of mitochondrial respiration decline progressively with irradiance (Buckley et al., 2017). In fact, the degree of inhibition of respiration in the light may reflect a strong plasticity of the respiratory system in C3 plants. Comparison of this flexibility among C3 plants is needed, and the gas-exchange system presented here can contribute physiological information for future investigations.

CONCLUSION

We have presented a method that allows the standard gas-exchange techniques to be extended to the measurement of NOP and GOP. With this method, a broad suite of gas-exchange properties can be measured while regulating light, CO_2, O_2, temperature, and humidity. The light response curves presented here were used to demonstrate the method and to determine several key parameters that could help improve our understanding of fundamental leaf processes. Two significant insights are highlighted. First, mitochondrial respiration was not inhibited in the light when leaves of French bean were exposed to nonphotorespiratory conditions. This result reinforces some earlier conclusions that photorespiration could indirectly play a major role in regulating the intensity of the Kok effect in some plants, but it remains to be further investigated. Second, g_m increases with an increase in light intensity. g_m inferred from O_2 fluxes represents an alternative and complementary approach that may clarify uncertainties in its measurement. For example, Farquhar and Busch (2017) demonstrated that the uncertainty associated with the measurement of respiration in the light using the Kok effect is of the same order of magnitude as the uncertainty in C_c using conventional CO_2 gas exchanges. Comparable calculations using the O_2 method are currently missing, and a better understanding of the limitations of O_2 diffusion toward the chloroplast is needed. Major uncertainties remain around the nature of the Kok effect and g_m. Measuring O_2 fluxes could add useful information to compute more accurate C_c values and thus examine the Kok effect with sufficient precision (Tcherkez et al., 2017a, 2017b). Finally, this technique creates opportunities to study the long-term response of gross photosynthesis to environmental changes and to investigate the balance between photochemical energy production by the electron transport chain and the utilization of this energy for carbon assimilation and other cell processes.

MATERIALS AND METHODS

Plant Material

Seeds of French bean (*Phaseolus vulgaris*) were germinated on wet filter paper in petri dishes for 5 to 6 d in the laboratory. Once true leaves appeared, plantlets were transferred to a greenhouse and placed in trays containing potting mix for 1 week before being transferred to 10-L pots. Photosynthetic photon flux density during a 16-h photoperiod was maintained above 500 μmol m^{-2} s^{-1} using supplemental high-pressure sodium lighting. Ambient temperature was maintained at approximately 23°C/14°C day/night. All pots were watered for 5 to 10 min, two to three times per day depending on plant size, by drip irrigation. Nutrient solution (Miracle-Gro enriched with iron-EDTA; Scotts) was applied twice per week. Mature green leaves (approximately 3 to 4 weeks old) were detached from the plants under water, and the apical leaflet was used for the experiment.

Gas-Exchange System

Gas-exchange measurements were made on fully expanded leaves placed in a glass and aluminum chamber similar to that described by von Caemmerer and Hubick (1989). The chamber's internal dimensions were 150 × 190 × 15 mm for a volume of 427.5 cm^3. The air within the chamber was well mixed with a 15-cm-long cross-flow fan driven by an external DC-powered, magnetically coupled drive (MagneDrive; Autoclave Engineers). The upper surface of the cuvette was sealed with a 10-mm-thick tempered glass plate measuring 170 × 260 mm. An air-tight seal was achieved by pressing the glass lid against a Viton O-ring with eight clamps to apply homogenous pressure. Air temperature inside the chamber was controlled by a thermoelectric (Peltier) temperature controller (TC-36-25; TE Technology) in thermal contact with the bottom of the cuvette. Two type K thermocouples coupled to amplifier breakout boards (MAX31850K; Adafruit Industries), interfaced to an Arduino Uno R3 (http://arduino.cc), were used to record air and leaf temperatures. The cuvette was uniformly illuminated by three controllable customized SPYDRx LED systems (Fluence Bioengineering) placed above the chamber. A small quantum sensor (Versatile Mini; Heinz Walz) inside the cuvette was used to measure PAR reaching the adaxial side of the leaf.

During each experiment, a constant flow of compressed air entered the chamber after passing through two Drierite columns (W.A. Hammond Drierite) and a glass cryogenic trap (at −50°C) to remove moisture. Some air exiting the chamber also was dried. A schematic of the gas-exchange system is presented in Figure 6. Dried compressed air was allowed to flow through a glass capillary into the reference side of the changeover valve of the mass spectrometer (Finnigan Delta plus XP; Fig. 6). A mass-flow meter (Aalborg) was used to measure the flow rate of air exiting the chamber. A second small fraction of exiting air was sent to an isotopic H_2O CRDS (L2130-I; Picarro) for analysis of the H_2O mixing ratio in air (Supplemental Figs. S6 and S7C) and $\delta^{18}O$ of water vapor ($\delta^{18}O_v$; Supplemental Figs. S6 and S7D). Transpiration rate (E) and g_s were calculated according to Buck (1981) and von Caemmerer and Farquhar (1981). Exiting air that was not sent to the water analyzer was dried by passage through a Drierite column and a glass water trap. A fraction of this air was sent to a CRDS CO_2 analyzer, which measured CO_2 (Supplemental Figs. S6 and S7A) and $\delta^{13}C$ in CO_2 (Supplemental Figs. S6 and S7A). Note that the $\delta^{13}C$ data were not used in any of the calculations of this article. A separate fraction of dried exiting air flowed through a glass capillary tube to the sample side of the mass spectrometer to measure $\delta O_2/N_2$ and $\delta^{18}O$ of O_2 (Supplemental Figs. S6 and S7, B and E, respectively).

Petiole Box

For each experiment, the leaf's petiole was placed in a 40- × 30- × 20-mm sealed aluminum box containing 22 cm^3 of ^{18}O-labeled water. The entire leaf and petiole box was placed inside the leaf chamber. In this way, any potential leak caused by the petiole or leaf blade crossing the side wall of the chamber was avoided (as described previously by von Caemmerer and Hubick [1989]

and Yakir et al. [1994]). The aluminum lid of the petiole box had a 10- × 10-mm aperture that allowed for the passage of the petiole. Underneath the lid, a 38- × 28- × 1-mm Viton sheet with smaller aperture was custom fit to the variable diameter of each leaf's petiole. The aluminum plate and Viton sheet suppressed evaporation from the petiole box to the point where it did not have a discernible influence on the concentration or $\delta^{18}O$ of water vapor exiting the cuvette. Thus, transpiration was the only significant source of water vapor (v) leaving the cuvette.

Leaf Water Labeling

An entire fully expanded leaf was detached from a plant, and the petiole was immediately immersed in tap water. The petiole was then recut under water to remove any potential embolism. After 30 min in darkness, the side leaflets were removed and the apical leaflet was used in the experiment. The leaf was transferred to the petiole box filled with labeled water (as described above) at 8,806‰ and 8,735‰ $\delta^{18}O$ for 21% O_2 and 2% O_2 experiments, respectively. The petiole was again recut under water inside the box, and the entire system (leaf + petiole box) was sealed inside the chamber. The course of leaf water labeling was followed using the CRDS (Fig. 6) to measure $\delta^{18}O_v$ of transpired water vapor exiting the chamber (Supplemental Figs. S6 and S7D).

Calculating GOP, NOP, and O_2 Uptake

GOP is defined as the rate of O_2 production by water splitting and NOP as the sum of all O_2 fluxes between air and the leaf. The $\delta^{18}O$ of leaf water ($\delta^{18}O_L$) is calculated first. Leaf water is the substrate for photosynthesis, and the $\delta^{18}O$ of photosynthetic O_2 approximates $\delta^{18}O_L$ (Guy et al., 1987). Mass balance equations constrain GOP and NOP, given the observed production rate of the two major isotopologues of O_2, $^{16}O_2$ and $^{18}O^{16}O$. O_2 uptake is then calculated by difference. Other isotopologues of O_2 have very low abundances, make a trivial contribution to O_2 fluxes, and are neglected. Errors introduced in GOP by this neglect are 0.04% for $^{17}O^{16}O$ and less for the less abundant $^{17}O_2$, $^{18}O^{17}O$, and $^{18}O_2$.

Air is run through the cuvette until $\delta^{18}O$ of water vapor exiting the chamber reaches a constant value, at which point the water balance is at steady state. Then, the isotopic composition of water entering the leaf through the petiole should be similar to that of water exiting the leaf through the transpiration stream. Thus, the flux of $H_2{}^{18}O$ derived from transpiration (i.e. $F_{18O\text{-}v}$), is calculated as:

$$F_{^{18}O-v} = F_{^{16}O-v}\left(\frac{H_2{}^{18}0}{H_2{}^{16}0}\right)_v \quad (1)$$

However, the $H_2{}^{18}O/H_2{}^{16}O$ ratio of water vapor (v) is less than its liquid source due to kinetic and equilibrium isotope fractionation during evaporation (Harwood et al., 1998). Applying the standard Craig-Gordon model of evaporation (Farquhar et al., 1989):

$$R_e = \alpha^+(\alpha_k R_s(1-h) + R_v h) \quad (2)$$

where R_e is the isotopic ratio at the site of evaporation, R_s is the isotopic ratio of the source of water (here, xylem), R_v is the isotopic ratio of the water vapor, α^+ is the equilibrium isotope fractionation at the leaf temperature (1.009; Majoube 1971), α_k is the kinetic isotope effect for the evaporation of water from the leaf into dry air (1.032; Cernusak et al., 2016), and h is relative humidity.

We initiated the measurement of the light response after 5 to 6 h at maximum illumination, when the $\delta^{18}O$ of transpired water reached an asymptotic value. We assumed that the leaf was at steady state, and so the water entering by the petiole is equivalent to the water exiting the leaf, in this case, $R_s = R_v$.

We further assumed that the water at the site of evaporation is a good representation of bulk leaf water, such that $R_e = R_{leaf}$, where R_{leaf} is the isotopic ratio of leaf water. Here, the $^{18}O/^{16}O$ ratio of H_2O will be represented as $\left(\frac{H_2{}^{18}O}{H_2{}^{16}O}\right)$, and so $R_v = \left(\frac{H_2{}^{18}O}{H_2{}^{16}O}\right)_v$ and $R_{leaf} = \left(\frac{H_2{}^{18}O}{H_2{}^{16}O}\right)_L$

Equation 2 can now be rearranged and solved for the ratio of $H_2{}^{18}O/H_2{}^{16}O$ in the evaporating liquid (leaf water) as a function of the ratio in the vapor, the kinetic and equilibrium O isotope fractionations, and the humidity:

$$\left(\frac{H_2{}^{18}O}{H_2{}^{16}O}\right)_L = \left(\frac{H_2{}^{18}O}{H_2{}^{16}O}\right)_v \alpha^+(\alpha_k + (1-\alpha_k)h) \quad (3)$$

$(H_2{}^{18}O/H_2{}^{16}O)_v$ is the ratio of water vapor measured by the CRDS in the air exiting the chamber. This equation shows that the $H_2{}^{18}O/H_2{}^{16}O$ of the liquid will be 1% to 2% higher than the ratio in the vapor, regardless of whether water entering the petiole is labeled. When calculating the gross rate of photosynthesis, this leaf water enrichment is taken into account.

The basic mass balance equation for O_2 and its major isotopologues ($^{16}O_2$ and $^{18}O^{16}O$) flowing through the cuvette is:

$$F_{O_{2\ out}} - F_{O_{2\ in}} = GOP - U_{^{16}O_2} \quad (4)$$

where GOP is gross O_2 production and U is O_2 uptake by respiration, photorespiration, and all other processes. To distinguish this flux from individual isotope fluxes, the production of each isotopologue will be represented by P.

An analogous equation can be written for $^{16}O_2$:

$$F_{^{16}O_{2out}} - F_{^{16}O_{2in}} = P_{^{16}O_{2in}} - U_{^{16}O_2} \quad (5)$$

In calculating O_2 fluxes, we consider only two isotopologues, $^{16}O_2$ and $^{18}O^{16}O$. The ratio of $^{18}O^{16}O/^{16}O_2$ is nominally 1:250. We do not consider $^{18}O_2$ because its abundance is so low ($^{18}O_2/^{16}O_2 \sim 1{:}250{,}000$). Equation 5 can be expanded to:

$$F_{^{18}O^{16}O_{out}} - F_{^{18}O^{16}O_{in}} = 2\left(\frac{H_2{}^{18}O}{H_2{}^{16}O}\right)_L P_{^{16}O_2} - \left(\frac{^{18}O^{16}O}{^{16}O_2}\right)_{cuv} U_{O_2}\alpha_U \quad (6)$$

The factor of 2 in the first term on the right-hand side reflects the fact that an O_2 molecule has two chances to acquire an ^{18}O atom from water splitting. The subscript cuv indicates ambient air inside the cuvette. The term α_U represents the isotope effect associated with respiration and all other uptake processes (photorespiration, alternative pathway, Mehler reaction…). Calculated fluxes are essentially insensitive to α_U (0.982), because the $\delta^{18}O$ of photosynthetic O_2 differs from that of ambient O_2 more than the $\delta^{18}O$ of O_2 consumed by respiration.

Solving Equation 5 for U_{16O2}, substituting into Equation 6, and solving for P_{16O2} gives:

$$P_{^{16}O_2} = \frac{\Delta F_{^{18}O^{16}O} - \left(\frac{^{18}O^{16}O}{^{16}O_2}\right)\alpha_U \Delta F_{^{16}O_2}}{2\left(\frac{H_2{}^{18}O}{H_2{}^{16}O}\right)_L - \left(\frac{^{18}O^{16}O}{^{16}O_2}\right)_{cuv}\alpha_U} \quad (7)$$

In Equation 7, $H_2{}^{18}O/H_2{}^{16}O_L = (H_2{}^{18}O/H_2{}^{16}O_{VSMOW})(1 + \delta^{18}O_{\text{-VSMOW}}/10^3)$ and $^{18}O^{16}O/^{16}O_{2cuv} = 2(H_2{}^{18}O/H_2{}^{16}O_{VSMOW})(1 + \delta^{18}O_{air\text{-}VSMOW}/10^3)(1 + \delta^{18}O_{cuv\text{-}air}/10^3)$. The subscripts air and cuv refer to O_2 in ambient air and air within the cuvette, respectively, as above. VSMOW indicates that the isotopic composition is expressed with Vienna Standard Mean Ocean Water as the reference. ΔF is the flux out of the chamber minus the flux into the chamber. This flux is the flux of $^{16}O_2$ or $^{18}O^{16}O$ out of the chamber minus the flux in. These fluxes are calculated from the change in $^{16}O_2/^{14}N_2$ and $^{18}O^{16}O/^{14}N_2$ as air passes through the cuvette, measured by the IRMS. In calculating these fluxes, we assume that the N_2 concentration of entering and exiting air is the same, the O_2 mixing ratio of air is 0.0201784, and the $^{18}O^{16}O/^{16}O_2$ ratio of ambient air is 0.0040104.

Considering that $(1 + {}^{18}O/{}^{16}O)^2$ is very close to 1, the production of $^{18}O_2$ (and other isotopologues) is negligible and the GOP is:

$$GOP = P_{^{16}O_2}\left[1 + 2\left(\frac{H_2{}^{18}O}{H_2{}^{16}O}\right)_L\right] \quad (8)$$

NOP is simply the sum of the outgoing minus incoming fluxes of $^{16}O_2$ (Eq. 5) and $^{18}O^{16}O$ (Eq. 6):

$$NOP = \Delta F_{^{16}O_2} + \Delta F_{^{18}O^{16}O} \quad (9)$$

The difference between outgoing and incoming fluxes of $^{16}O_2$ is determined using $\delta O_2/N_2$ (see below). Net O_2 uptake is the difference between GOP and NOP (GOP − NOP).

Mass Spectrometric Measurements of GOP and NOP

To determine GOP and NOP, we used a Thermo Delta plus XP IRMS (Thermo Finnigan) configured to simultaneously measure masses 28, 29, 32, 33, 34, 38, 40, and 44. The changeover valve of the mass spectrometer was connected to the gas-exchange system using two 25-μm-i.d. glass capillaries (SGE Analytical Science). The connections of the capillaries with the chamber and the changeover valve were secured with vespal ferrules (Agilent Technologies). To equalize sample and reference side ion currents, the capillary length was set to 149 cm on the sample side and to 145 cm on the reference side. Each measurement consisted of a block of 16 to 25 cycles (reference/sample/reference changeovers).

For each cycle, $\delta O_2/N_2$ (32/28) and $\delta^{18}O$ of O_2 (34/32) were calculated from the difference in isotope ratios of air leaving and entering the cuvette. Both elemental and isotopic ratios were expressed in the standard δ notation as:

$$\delta(‰) = 1000\left(\frac{Ratio_{sample}}{Ratio_{reference}} - 1\right) \quad (10)$$

$Ratio_{sample}$ and $Ratio_{reference}$ are the measured ion current ratios of $^{16}O_2/^{14}N_2$ and $^{18}O^{16}O/^{16}O_2$.

Light Response Curves

Light response curves of net CO_2 assimilation, NOP, and GOP were obtained by decreasing PAR measured at the top of the leaf from high light to darkness. Typical data collected from an experiment at 21% O_2 are presented in Figure 1, based on results from 10 decreasing light levels (1,100, 800, 500, 200, 100, 80, 70, 60, 40, and 0 μmol m^{-2} s^{-1}). Similar experiments were done using air containing 2% O_2 to minimize photorespiration. For the 2% O_2 experiments, maximal light intensity was reduced to 700 μmol m^{-2} s^{-1} and fluxes were measured at a greater number of lower light intensities (900, 700, 420, 300, 150, 100, 90, 80, 70, 60, 40, 35, and 0 μmol m^{-2} s^{-1}). Typical data collected from an experiment at 2% O_2 are presented in Figure 1. Light response curve data were fitted with the nonrectangular quadratic function of Ögren and Evans (1993) using the curve-fit routine of SciPy (Oliphant, 2007; Millman and Aivazis, 2011; van der Walt et al., 2011). This routine uses nonlinear least squares for the specified functional form.

Mesophyll Conductance

g_m was evaluated using the common approach of adopting a single resistance (g_m) to characterize the transport of CO_2 between the intercellular airspace and the site of carboxylation (Tholen et al., 2012). g_m was calculated using the O_2 equations developed by Renou et al. (1990). O_2 uptake (U) is given by the sum of the rate of Rubisco oxygenation (V_o), the rate of oxygen consumption by the oxidation of glycolate during the C_2 cycle ($0.5V_o$), and mitochondrial respiration and other processes (Mehler reaction, plastoquinone terminal oxidase…; designated as R_o):

$$U = V_o + 0.5\ V_o + R_o \quad (11)$$

A similar equation was developed from Farquhar et al. (1980) for CO_2 assimilation:

$$A_{net} = V_c - 0.5V_o - R_c \quad (12)$$

where V_c is the velocity of carboxylation and R_c is the rate of decarboxylation in the light associated with mitochondrial respiration. Solving Equation 11 for V_o, combining with Equation 12, and solving for V_c gives:

$$V_c = A_{net} + \frac{(U - R_o)}{3} + R_c \quad (13)$$

In addition, Farquhar and von Caemmerer (1982) defined C_c as:

$$C_c = 2\Gamma^*\left(\frac{V_c}{V_o}\right) \quad (14)$$

Γ^* is the CO_2 compensation point in the absence of respiration in the light. By combining Equations 13 and 14, we obtain:

$$C_c = \frac{\Gamma^*(3A_{net} + U - R_o + 3R_c)}{(U - R_o)} \quad (15)$$

The limitation of photosynthesis through g_m can be written, following Fick's law, as:

$$C_c = C_i - \frac{A_{net}}{g_m} \quad (16)$$

And so:

$$g_m = \frac{A_{net}(U - R_o)}{C_i(U - R_o) - \Gamma^*(3A_{net} + U - R_o + 3R_c)} \quad (17)$$

Here, Γ^* was not measured but assumed to be 42.75 μmol mol^{-1} at 25°C, as estimated by Bernacchi et al. (2001). A standardized Arrhenius function and assumed activation energy of 37.8 kJ mol^{-1} were used to account for the effect of temperature on Γ^*, as in Medlyn et al. (2002).

In the case where $R_c = R_o$, as assumed by Renou et al. (1990), Equation 17 can be simplified as in Flexas et al. (2012):

$$g_m = \frac{A_{net}(U - R)}{C_i(U - R) - \Gamma^*(3A_{net} + U + 2R)} \quad (18)$$

where R is respiration rate in the light.

Determining Terms Needed to Calculate g_m

The rate of respiration in the light (R) was determined by extrapolating the linear portion of the A_{net} versus irradiance curve to zero irradiance (Kok, 1948). It is important to note that this extrapolation assumes that it is possible to extrapolate from conditions where $C_c < C_a$, above the break point in the light response curve, to conditions where $C_c > C_a$, below the light compensation point. This approach to assessing the respiration rate in the light was challenged recently (Farquhar and Busch 2017; but see Buckley et al., 2017) but is provisionally retained.

The zero-irradiance intercepts of the light response curves of NOP were calculated from net C assimilation rates measured between 40 and 110 μmol m^{-2} s^{-1}. These values were then equated to both R_o and R_c. To account for the dependence of A_{net} or NOP on changes in internal CO_2 concentration, R_o and R_c were recalculated according to Kirschbaum and Farquhar (1987). This correction uses an estimate of the rate of ribulose 1,5-bisphosphate regeneration, V_j, calculated from A_{net} or NOP. It constrains R_c and R_o when the intercept of the linear regression of V_j versus light is zero. Uncorrected values are reported as R_o-apparent and R_c-apparent. Corrected values are reported as R_o-corrected and R_c-corrected. R_o-corrected and R_c-corrected values were used in Equations 11 and 12 and in all further calculations. The parameters V_j and R_o were used to correct NOP for variable C_i; V_j and R_c were used to correct A_{net}.

Typical Experimental Protocol

Before and during each experiment, the reference gas (incoming air) was analyzed against itself to assess the magnitude and drift in the zero enrichment (shaded areas in Supplemental Figs. S6 and S7). The zero enrichment is the artifactual difference in the composition of incoming and outgoing air when there is no source or sink for O_2 within the chamber. Leaves were initially placed in the dark for 30 min. The light intensity was then raised to maximize transpiration and accelerate leaf labeling. Leaves were maintained in this condition until $\delta^{18}O$ of the water vapor reached isotopic steady state. At this point, the $\delta^{18}O$ of transpired water leaving the chamber was constant (Supplemental Figs. S6 and S7D), and the measure of O_2 and CO_2 fluxes began, along with their light response, as described above. For the duration of an experiment, leaves were exposed to either 21% O_2 (Supplemental Fig. S6) or 2% O_2 (Supplemental Fig. S7) in air. Air temperature was maintained at 20°C ± 1°C. Averaged leaf area was 46.23 ± 1.3 and 81.06 ± 2.44 cm^2 at 21% O_2 and 2% O_2, respectively. Average flow rate was measured at 2.47 ± 0.1 and 2.64 ± 0.1 L min^{-1} at 21% O_2 and 2% O_2, respectively, under our typical conditions (1 atm pressure and 20°C ± 1°C).

Comparative Estimates of Photosynthetic Properties

Alternative formulations from the literature were used to calculate J_g and g_m in order to evaluate the accuracy of our calculations from GOP measurements. The theoretical electron transport rate, J_g, was calculated as by Flexas et al. (2012; Eq. 12.18):

$$J_g = (A + R_d)\frac{4(C_c + 2\Gamma^*)}{C_c - \Gamma^*} \quad (19)$$

C_c was arbitrarily calculated from ambient CO_2 exiting the chamber, C_a, as $C_c = 0.4\ C_a$ following Roupsard et al. (1996).

To determine the accuracy of g_m, theoretical g_m was calculated using Equation 7 from Harley et al. (1992), which considers a variable J (for review, see Flexas et al., 2012, and refs. therein):

$$g_m = \frac{A_{net}}{C_i - \frac{\Gamma^*(J_a + 8(A_{net} + R_c))}{J_a - 4(A_{net} + R_c)}} \quad (20)$$

Usually, J_a is obtained indirectly using fluorescence measurements. In the absence of such measurements, we assumed J_a = 4*GOP, as in von Caemmerer (2000),

since four electrons are produced for each molecule of O_2 released by PSII. This estimate of g_m is referred to as g_m Harley (Supplemental Figs. S2 and S3).

Statistical Analysis

Linear regressions were used to determine the linearity in the light response of NOP, GOP, and A_{net}. These regressions also were used to calculate the Kok effect. Uncertainties correspond to a confidence interval of 95%. Linear regressions also were used to determine the correlation of O_2 versus CO_2. Independent Student's t tests were used to assess the statistical difference between dark respiration and R_L values and between R_L values from A_{net} and NOP. Differences between means were considered significant at p-value < 0.05 and highly significant at p-value < 0.01.

Supplemental Data

The following supplemental materials are available.

Supplemental Figure S1. The variation of C_a and C_i with light intensity for French bean leaves exposed to 21% O_2 and 2% O_2.

Supplemental Figure S2. Correlation between g_m calculated using the O_2 method and theoretical g_m calculated using the variable J method of Harley et al. (1992).

Supplemental Figure S3. g_m versus irradiance for French bean leaves exposed to 21% O_2.

Supplemental Figure S4. $\delta O_2/N_2$, NOP, $\delta^{18}O$, and GOP for each of three replicate incubations versus irradiance for French bean leaves exposed to 21% O_2.

Supplemental Figure S5. $\delta O_2/N_2$, NOP, $\delta^{18}O$, and GOP for each of three replicate incubations versus irradiance for French bean leaves exposed to 2% O_2.

Supplemental Figure S6. Measurements for a French bean leaf exposed to 21% O_2.

Supplemental Figure S7. Measurements for a French bean leaf exposed to 2% O_2.

ACKNOWLEDGMENTS

We thank Guillaume Tcherkez, Joseph Berry, and Graham Farquhar for commentaries on an early version of this article. We also thank the anonymous reviewers for their valuable comments on the article, Robert Stevens for machining the aluminum chamber, and Karina Graeter for assisting with its design. P.P.G.G. thanks Jordan Lubkeman for technical assistance.

Received May 9, 2016; accepted March 5, 2018; published March 27, 2018.

LITERATURE CITED

André MJ (2011) Modelling $^{18}O_2$ and $^{16}O_2$ unidirectional fluxes in plants. II. Analysis of rubisco evolution. Biosystems **103:** 252–264

André MJ (2013) Modelling $^{18}O_2$ and $^{16}O_2$ unidirectional fluxes in plants. III. Fitting of experimental data by a simple model. Biosystems **113:** 104–114

Angert A, Muhr J, Negron Juarez R, Alegria Muñoz W, Kraemer G, Ramirez Santillan J, Barkan E, Mazeh S, Chambers JQ, Trumbore SE (2012) Internal respiration of Amazon tree stems greatly exceeds external CO_2 efflux. Biogeosciences **9:** 4979–4991

Atkin OK, Bruhn D, Hurry VM, Tjoelker MG (2005) The hot and the cold: unravelling the variable response of plant respiration to temperature. Funct Plant Biol **32:** 87–105

Atkins CA, Canvin DT (1971) Photosynthesis and CO_2 evolution by leaf discs: gas exchange, extraction, and ion-exchange fractionation of ^{14}C-labelled photosynthetic products. Can J Bot **49:** 1225–1234

Aubert S, Gout E, Bligny R, Marty-Mazars D, Barrieu F, Alabouvette J, Marty F, Douce R (1996) Ultrastructural and biochemical characterization of autophagy in higher plant cells subjected to carbon deprivation: control by the supply of mitochondria with respiratory substrates. J Cell Biol **133:** 1251–1263

Badger MR, von Caemmerer S, Ruuska S, Nakano H (2000) Electron flow to oxygen in higher plants and algae: rates and control of direct photoreduction (Mehler reaction) and rubisco oxygenase. Philos Trans R Soc Lond B Biol Sci **355:** 1433–1446

Bender ML, Battle M, Keeling RF (1998) The O_2 balance of the atmosphere: a tool for studying the fate of fossil-fuel CO_2. Energy Environ **23:** 207–223

Bender ML, Tans PP, Ellis TJ, Orchardo J, Habfast K (1994) A high precision isotope ratio mass spectrometry method for measuring the O_2N_2 ratio of air. Geochim Cosmochim Acta **58:** 4751–4758

Bernacchi CJ, Singsaas EL, Pimentel C, Portis AR, Long SP (2001) Improved temperature response functions for models of rubisco-limited photosynthesis. Plant Cell Environ **24:** 253–259

Berry JA, Osmond CB, Lorimer GH (1978) Fixation of $^{18}O_2$ during photorespiration: kinetic and steady-state studies of the photorespiratory carbon oxidation cycle with intact leaves and isolated chloroplasts of C3 plants. Plant Physiol **62:** 954–967

Biehler K, Fock H (1995) Estimation of non-cyclic electron transport in vivo of *Triticum* using chlorophyll fluorescence and mass spectrometric O_2 evolution. J Plant Physiol **145:** 422–426

Biehler K, Haupt-Herting S, Beckmann J, Fock H, Becker TW (1997) Simultaneous CO_2- and $^{16}O_2/^{18}O_2$-gas exchange and fluorescence measurements indicate differences in light energy dissipation between the wild type and the phytochrome-deficient aurea mutant of tomato during water stress. J Exp Bot **48:** 1439–1449

Bloom AJ, Caldwell RM, Finazzo J, Warner RL, Weissbart J (1989) Oxygen and carbon dioxide fluxes from barley shoots depend on nitrate assimilation. Plant Physiol **91:** 352–356

Buck AL (1981) New equations for computing vapor pressure and enhancement factor. J Appl Meteorol **20:** 1527–1532

Buckley TN (2017) Modeling stomatal conductance. Plant Physiol **174:** 572–582

Buckley TN, Farquhar GD, Mott KA (1997) Qualitative effects of patchy stomatal conductance distribution features on gas-exchange calculations. Plant Cell Environ **20:** 867–880

Buckley TN, Vice H, Adams MA (2017) The Kok effect in *Vicia faba* cannot be explained solely by changes in chloroplastic CO_2 concentration. New Phytol **216:** 1064–1071

Canvin DT, Berry JA, Badger MR, Fock H, Osmond CB (1980) Oxygen exchange in leaves in the light. Plant Physiol **66:** 302–307

Cernusak LA, Barbour MM, Arndt SK, Cheesman AW, English NB, Feild TS, Helliker BR, Holloway-Phillips MM, Holtum JA, Kahmen A, et al (2016) Stable isotopes in leaf water of terrestrial plants. Plant Cell Environ **39:** 1087–1102

Cornic G, Jarvis PG (1972) Effects of oxygen on CO_2 exchange and stomatal resistance in Sitka spruce and maize at low irradiances. Photosynthetica **6:** 225–239

Cornic G, Le Gouallec JL, Briantais JM, Hodges M (1989) Effect of dehydration and high light on photosynthesis of two C3 plants (*Phaseolus vulgaris* L. and *Elatostema repens* (Lour.) Hall f.). Planta **177:** 84–90

Devaux C, Baldet P, Joubès J, Dieuaide-Noubhani M, Just D, Chevalier C, Raymond P (2003) Physiological, biochemical and molecular analysis of sugar-starvation responses in tomato roots. J Exp Bot **54:** 1143–1151

Douthe C, Dreyer E, Brendel O, Warren CR (2012) Is mesophyll conductance to CO_2 in leaves of three Eucalyptus species sensitive to short-term changes of irradiance under ambient as well as low O_2? Funct Plant Biol **38:** 435–447

Douthe C, Dreyer E, Epron D, Warren CR (2011) Mesophyll conductance to CO_2, assessed from online TDL-AS records of $^{13}CO_2$ discrimination, displays small but significant short-term responses to CO_2 and irradiance in Eucalyptus seedlings. J Exp Bot **62:** 5335–5346

Evans JR, Sharkey TD, Berry JA, Farquhar GD (1986) Carbon isotope discrimination measured concurrently with gas exchange to investigate CO_2 diffusion in leaves of higher plants. Aust J Plant Physiol **13:** 281–292

Farquhar GD, Busch FA (2017) Changes in the chloroplastic CO_2 concentration explain much of the observed Kok effect: a model. New Phytol **214:** 570–584

Farquhar GD, Cernusak LA (2012) Ternary effects on the gas exchange of isotopologues of carbon dioxide. Plant Cell Environ **35:** 1221–1231

Farquhar GD, Ehleringer JR, Hubick KT (1989) Carbon isotope discrimination and photosynthesis. Annu Rev Plant Biol **40:** 503–537

Farquhar GD, von Caemmerer S (1982) Modelling of photosynthetic response to environmental conditions. *In* OL Lange, PS Nobel, CB Osmond, H Ziegler, eds, Physiological Plant Ecology II. Encyclopedia of Plant Physiology (New Series), **Vol 12/B**. Springer, Berlin, pp 549–587

Farquhar GD, von Caemmerer S, Berry JA (1980) A biochemical model of photosynthetic CO_2 assimilation in leaves of C3 species. Planta **149:** 78–90

Flexas J, Bota J, Galmes J, Medrano H, Ribas-Carbo M (2006) Keeping a positive carbon balance under adverse conditions: responses of photosynthesis and respiration to water stress. Physiol Plant **127:** 343–352

Flexas J, Diaz-Espejo A, Galmés J, Kaldenhoff R, Medrano H, Ribas-Carbo M (2007) Rapid variations of mesophyll conductance in response to changes in CO_2 concentration around leaves. Plant Cell Environ **30:** 1284–1298

Flexas J, Loreto F, Medrano H (2012) Terrestrial Photosynthesis in a Changing Environment: A Molecular, Physiological, and Ecological Approach. Cambridge University Press, Cambridge, UK

Furbank RT, Badger MR, Osmond CB (1982) Photosynthetic oxygen exchange in isolated cells and chloroplasts of C3 plants. Plant Physiol **70:** 927–931

Gauthier PPG, Bligny R, Gout E, Mahé A, Nogués S, Hodges M, Tcherkez GGB (2010) In folio isotopic tracing demonstrates that nitrogen assimilation into glutamate is mostly independent from current CO_2 assimilation in illuminated leaves of *Brassica napus*. New Phytol **185:** 988–999

Genty B, Briantais JM, Baker NR (1989) The relationship between the quantum yield of photosynthetic electron transport and quenching of chlorophyll fluorescence. Biochim Biophys Acta **990:** 87–92

Gerbaud A, André M (1979) Photosynthesis and photorespiration in whole plants of wheat. Plant Physiol **64:** 735–738

Goldman JA, Kranz SA, Young JN, Tortell PD, Stanley RH, Bender ML, Morel FM (2015) Gross and net production during the spring bloom along the Western Antarctic Peninsula. New Phytol **205:** 182–191

Gong XY, Schäufele R, Feneis W, Schnyder H (2015) $^{13}CO_2/^{12}CO_2$ exchange fluxes in a clamp-on leaf cuvette: disentangling artefacts and flux components. Plant Cell Environ **38:** 2417–2432

Grande KD, Marra J, Langdon C, Heinemann K, Bender ML (1989) Rates of respiration in the light measured in marine phytoplankton using an ^{18}O isotope-labelling technique. J Exp Mar Biol Ecol **129:** 95–120

Griffin KL, Turnbull MH (2013) Light saturated RuBP oxygenation by Rubisco is a robust predictor of light inhibition of respiration in *Triticum aestivum* L. Plant Biol (Stuttg) **15:** 769–775

Guy RD, Fogel MF, Berry JA, Hoering TC (1987) Isotope fractionation during oxygen production and consumption by plants. *In* J Biggins, eds, Progress in Photosynthesis Research. Springer, Dordrecht, The Netherlands, pp 597–600

Hagemann M, Fernie AR, Espie GS, Kern R, Eisenhut M, Reumann S, Bauwe H, Weber APM (2013) Evolution of the biochemistry of the photorespiratory C_2 cycle. Plant Biol (Stuttg) **15:** 639–647

Harley PC, Loreto F, Di Marco G, Sharkey TD (1992) Theoretical considerations when estimating the mesophyll conductance to CO_2 flux by analysis of the response of photosynthesis to CO_2. Plant Physiol **98:** 1429–1436

Harris GC, Cheesbrough JK, Walker DA (1983) Effects of mannose on photosynthetic gas exchange in spinach leaf discs. Plant Physiol **71:** 108–111

Harwood KG, Gillon JS, Griffiths H, Broadmeadow MSJ (1998) Diurnal variation of $\Delta^{13}CO_2$, $\Delta C^{18}O^{16}O$ and evaporative site enrichment of $\delta H_2{}^{18}O$ in *Piper aduncum* under field conditions in Trinidad. Plant Cell Environ **21:** 269–283

Hassiotou F, Ludwig M, Renton M, Veneklaas EJ, Evans JR (2009) Influence of leaf dry mass per area, CO_2, and irradiance on mesophyll conductance in sclerophylls. J Exp Bot **60:** 2303–2314

Haupt-Herting S, Fock HP (2000) Exchange of oxygen and its role in energy dissipation during drought stress in tomato plants. Physiol Plant **110:** 489–495

Haupt-Herting S, Fock HP (2002) Oxygen exchange in relation to carbon assimilation in water-stressed leaves during photosynthesis. Ann Bot **89:** 851–859

Heskel MA, Atkin OK, Turnbull MH, Griffin KL (2013) Bringing the Kok effect to light: a review on the integration of daytime respiration and net ecosystem exchange. Ecosphere **4:** 1–14

Hillier W (2008) The significance of O2 for biology. *In* SE Jorgensen, B Fath, eds, Encyclopedia of Ecology. Elsevier, pp 3543–3550

Hoch G, Owens OV, Kok B (1963) Photosynthesis and respiration. Arch Biochem Biophys **101:** 171–180

Ishii R, Murata Y (1978) Further evidence of the Kok effects in C3 plants and the effects of environmental factors on it. Jpn J Crop Sci **47:** 547–550

Kirschbaum MU, Farquhar GD (1987) Investigation of the CO_2 dependence of quantum yield and respiration in *Eucalyptus pauciflora*. Plant Physiol **83:** 1032–1036

Kok B (1948) A critical consideration of the quantum yield of *Chlorella* photosynthesis. Enzymologia **13:** 1–56

Kok B (1956) On the inhibition of photosynthesis by intense light. Biochim Biophys Acta **21:** 234–244

Laisk A, Kiirats O, Oja V, Gerst U, Weis E, Heber U (1992) Analysis of oxygen evolution during photosynthetic induction and in multiple-turnover flashes in sunflower leaves. Planta **186:** 434–441

Laisk A, Oja V (1998) Dynamics of Leaf Photosynthesis: Rapid-Response Measurements and Their Interpretations. CSIRO Publishing, Collingwood, Australia

Majoube M (1971) Fractionnement en oxygene 18 et en deuterium entre l'eau et sa vapeur. J Chim Phys **68:** 1423–1436

Medlyn BE, Dreyer E, Ellsworth D, Forstreuter M, Harley PC, Kirschbaum MUF, Le Roux X, Montpied P, Strassemeyer J, Walcroft A, et al (2002) Temperature response of parameters of a biochemically based model of photosynthesis. II. A review of experimental data. Plant Cell Environ **25:** 1167–1179

Mehler AH, Brown AH (1952) Studies on reactions of illuminated chloroplasts. III. Simultaneous photoproduction and consumption of oxygen studied with oxygen isotopes. Arch Biochem Biophys **38:** 365–370

Millman KJ, Aivazis M (2011) Python for scientists and engineers. Comput Sci Eng **13:** 9–12

Mott KA, Buckley TN (2000) Patchy stomatal conductance: emergent collective behaviour of stomata. Trends Plant Sci **5:** 258–262

Nogués S, Tcherkez G, Cornic G, Ghashghaie J (2004) Respiratory carbon metabolism following illumination in intact French bean leaves using 13C/12C isotope labeling. Plant physiology **136:** 3245–3254.

Ögren E, Evans JR (1993) Photosynthetic light-response curves. Planta **189:** 182–190

Oja V, Eichelmann H, Laisk A (2007) Calibration of simultaneous measurements of photosynthetic carbon dioxide uptake and oxygen evolution in leaves. Plant Cell Physiol **48:** 198–203

Oliphant TE (2007) Python for scientific computing. Comput Sci Eng **9:** 10–20

Ozbun JL, Volk RJ, Jackson WA (1964) Effects of light and darkness on gaseous exchange of bean leaves. Plant Physiol **39:** 523–527

Peltier G, Thibault P (1985) O_2 uptake in the light in *Chlamydomonas*: evidence for persistent mitochondrial respiration. Plant Physiol **79:** 225–230

Radmer R, Ollinger O (1980) Light-driven uptake of oxygen, carbon dioxide, and bicarbonate by the green alga *Scenedesmus*. Plant Physiol **65:** 723–729

Renou JL, Gerbaud A, Just D, André M (1990) Differing substomatal and chloroplastic CO_2 concentrations in water-stressed wheat. Planta **182:** 415–419

Roupsard O, Gross P, Dreyer E (1996) Limitation of photosynthetic activity by CO_2 availability in the chloroplasts of oak leaves from different species and during drought. Ann Sci For **53:** 243–254

Ruuska SA, Badger MR, Andrews TJ, von Caemmerer S (2000) Photosynthetic electron sinks in transgenic tobacco with reduced amounts of Rubisco: little evidence for significant Mehler reaction. J Exp Bot **51:** 357–368

Sage RF, Cen YP, Li M (2002) The activation state of Rubisco directly limits photosynthesis at low CO_2 and low O_2 partial pressures. Photosynth Res **71:** 241–250

Savvides A, Fanourakis D, van Ieperen W (2012) Co-ordination of hydraulic and stomatal conductances across light qualities in cucumber leaves. J Exp Bot **63:** 1135–1143

Singsaas EL, Ort DR, DeLucia EH (2001) Variation in measured values of photosynthetic quantum yield in ecophysiological studies. Oecologia **128:** 15–23

Sharp RE, Matthews MA, Boyer JS (1984) Kok effect and the quantum yield of photosynthesis: light partially inhibits dark respiration. Plant Physiol **75:** 95–101

Tazoe Y, von Caemmerer S, Badger MR, Evans JR (2009) Light and CO_2 do not affect the mesophyll conductance to CO_2 diffusion in wheat leaves. J Exp Bot **60:** 2291–2301

Tazoe Y, von Caemmerer S, Estavillo GM, Evans JR (2011) Using tunable diode laser spectroscopy to measure carbon isotope discrimination and mesophyll conductance to CO_2 diffusion dynamically at different CO_2 concentrations. Plant Cell Environ **34:** 580–591

Tcherkez G, Bligny R, Gout E, Mahé A, Hodges M, Cornic G (2008) Respiratory metabolism of illuminated leaves depends on CO_2 and O_2 conditions. Proc Natl Acad Sci USA **105:** 797–802

Tcherkez G, Gauthier P, Buckley TN, Busch FA, Barbour MM, Bruhn D, Heskel MA, Gong XY, Crous K, Griffin K, et al (2017b) Leaf day respiration: low CO_2 flux but high significance for metabolism and carbon balance. New Phytol **216:** 986–1001

Tcherkez G, Nogués S, Bleton J, Cornic G, Badeck F, Ghashghaie J (2003) Metabolic origin of carbon isotope composition of leaf dark-respired CO_2 in French bean. Plant Physiol **131:** 237–244

Tholen D, Ethier G, Genty B, Pepin S, Zhu XG (2012) Variable mesophyll conductance revisited: theoretical background and experimental implications. Plant Cell Environ **35:** 2087–2103

Tombesi S, Nardini A, Farinelli D, Palliotti A (2014) Relationships between stomatal behavior, xylem vulnerability to cavitation and leaf water relations in two cultivars of *Vitis vinifera*. Physiol Plant **152:** 453–464

van der Walt S, Colbert SC, Varoquaux G (2011) The Numpy array: a structure for efficient numerical computation. Comput Sci Eng **13:** 22–30

von Caemmerer S, Farquhar GD (1981) Some relationships between the biochemistry of photosynthesis and the gas exchange of leaves. Planta **153:** 376–387

von Caemmerer S, Hubick KT (1989) Short-term carbon-isotope discrimination in C3-C4 intermediate species. Planta **178:** 475–481

Von Caemmerer S (2000) Biochemical models of leaf photosynthesis. CSIRO Publishing, Australia

Xiong D, Liu X, Liu L, Douthe C, Li Y, Peng S, Huang J (2015) Rapid responses of mesophyll conductance to changes of CO_2 concentration, temperature and irradiance are affected by N supplements in rice. Plant Cell Environ **38:** 2541–2550

Yakir D (1992) Variations in the natural abundance of oxygen-18 and deuterium in plant carbohydrates. Plant Cell Environ **15:** 1005–1020

Yakir D, Berry JA, Giles L, Osmond CB (1994) Isotopic heterogeneity of water in transpiring leaves: identification of the component that controls the $\delta^{18}O$ of atmospheric O_2 and CO_2. Plant Cell Environ **17:** 73–80

Yin X, Sun Z, Struik PC, Gu J (2011) Evaluating a new method to estimate the rate of leaf respiration in the light by analysis of combined gas exchange and chlorophyll fluorescence measurements. J Exp Bot **62:** 3489–3499